

# Synthesis and Characterization of Dense and Porous Cellulose Films

Vivek P. Khare,<sup>1</sup> Alan R. Greenberg,<sup>1</sup> Stephen S. Kelley,<sup>2</sup> Heidi Pilath,<sup>2</sup> Il Juhn Roh,<sup>3</sup> Jeff Tyber<sup>1</sup>

<sup>1</sup>Department of Mechanical Engineering, NSF Membrane Applied Science and Technology Center, University of Colorado at Boulder, Boulder, Colorado 80309-0427

<sup>2</sup>National Renewable Energy Laboratory, Golden Colorado 80401-3393

<sup>3</sup>Hydranautics, Inc., 401 Jones Road, Oceanside, California 92054

Received 30 March 2005; accepted 7 November 2005

DOI 10.1002/app.25888

Published online 13 April 2007 in Wiley InterScience (www.interscience.wiley.com).

**ABSTRACT:** Whereas cellulose-derived polymers are routinely used as membrane materials, the cellulose polymer itself is not directly used to synthesize dense/porous films for membrane applications. Recently, *N*-methylmorpholine *N*-oxide (NMMO) and dimethylacetamide (DMAc)/lithium chloride (LiCl) have been successfully employed for dissolving unmodified cellulose. This provides a strong rationale for reexamining the possibility of cellulose membrane fabrication using these solvents. By judiciously selecting solvents, casting conditions, and solvent exchange steps, we successfully synthesized dense/asymmetric-porous cellulose films. The pore size and porosity of the porous films decreased systematically with increasing cellulose concentration. SEM analysis of the cross sections revealed an asymmetric skinned structure with monotonically increasing pore size away from the

skin. The measured pore diameters were in the range 1.8–4.8  $\mu\text{m}$ . Mechanical testing indicated that the dense films possessed tensile properties comparable to those of cellulose acetate (CA) films. Though nitrogen permeability values were comparable for cellulose and CA dense films, cellulose film permeability depended upon the type of drying protocol employed. Overall, these results demonstrate that processability need not be a constraint in the use of cellulose polymer for membrane fabrication. In selected applications, cellulose membranes could become a cost-effective, environmentally friendly alternative to other more commonly employed membrane polymers. © 2007 Wiley Periodicals, Inc. *J Appl Polym Sci* 105: 1228–1236, 2007

**Key words:** membranes; cellulose; microfiltration; ultrafiltration; porous film characterization

## INTRODUCTION

Cellulose derivatives such as cellulose acetate (CA), cellulose triacetate (CTA), and cellulose nitrate (CN) are routinely and extensively used as membrane materials. For example, CA membranes are used in gas separation, reverse osmosis (RO), ultrafiltration (UF), and microfiltration (MF);<sup>1–3</sup> CTA membranes are used in RO and UF;<sup>1,2</sup> and CN membranes are used in MF applications.<sup>1</sup> These membranes are typically made using phase inversion techniques whereby a solution containing the polymer is cast in the desired shape, and phase inversion is effected by incorporation of a nonsolvent, removal of the solvent, or by changing the temperature of the polymer solution. The ability to obtain a moderately viscous homogeneous polymer solution is an important precondition to such membrane formation techniques. CA, CTA, and CN readily dissolve in numerous ketone and ester solvents such as acetone, methyl

acetate, and polar aprotic solvents such as dimethyl acetamide (DMAc), *n*-methyl pyrrolidone (NMP), and dimethyl sulfoxide (DMSO).<sup>4</sup> As is well recognized, a variety of membrane microstructures can be prepared from these cellulose derivatives.

Unlike the cellulose derivatives, the cellulose polymer itself is not viewed as a good membrane material because its unique structure (Fig. 1) severely limits the processability of the cellulose polymer. Cellulose is a polysaccharide composed of glucosidic rings linked through oxygen bridges with a repeat unit having three hydroxyl groups and an acetal linkage. Strong hydrogen bonding between the hydroxyl groups make cellulose a highly crystalline, insoluble polymer that degrades before melting.<sup>5,6</sup> Since cellulose is not soluble in common solvents, casting by standard methods is not possible and the relatively low degradation temperature precludes melt processing.<sup>6</sup>

From a broader perspective, cellulose is a relatively inexpensive, biodegradable, and sustainable polymer. Hence, there is a strong rationale to use the cellulose polymer itself as a raw material for making porous and dense membranes. Since the early 1990s, new processes based on organic solvents—

Correspondence to: V. P. Khare (vivek.khare1@ge.com).

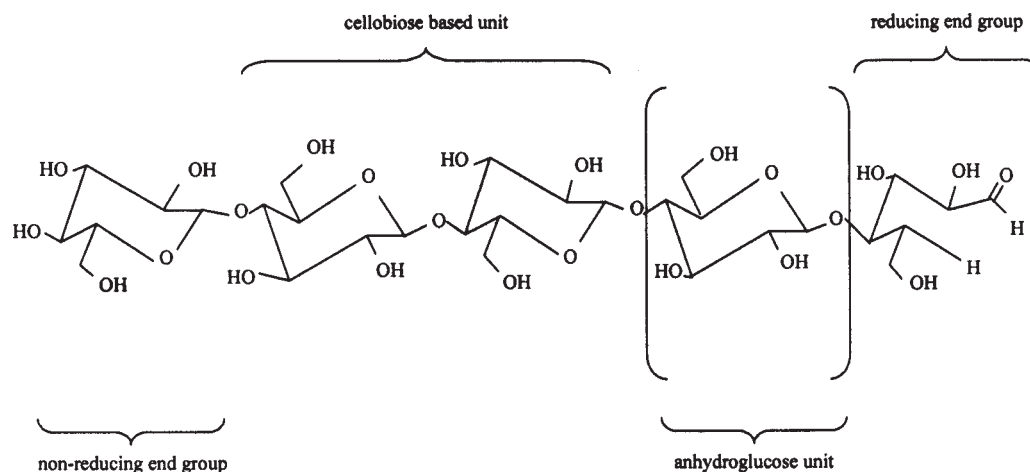


**Figure 1** Molecular structure of cellulose. Cellulose is a linear syndiotactic homopolymer composed of D-anhydroglucopyranose units (AGU) linked together by  $\beta$ -(1 $\rightarrow$ 4)-glycosidic bonds. If the dimer cellobiose is considered as the basic unit, then cellulose can be considered as an isotactic polymer of cellobiose.

*N*-methylmorpholine *N*-oxide (NMMO) and dimethylacetamide (DMAc)/lithium chloride (LiCl)—and more recently ionic liquids such as 1-butyl-3-methylimidazolium chloride have been explored to produce regenerated cellulose films.<sup>7,8</sup> The use of such solvents for making cellulose films and fibers has several important advantages. Since cellulose dissolution involves purely physical unit operations, no chemical byproducts requiring disposal as waste products are formed. Moreover, the solvents can be recycled completely, which makes the cellulose-dissolution-based processes environmentally friendly. Not surprisingly, the dissolution-based processes are increasingly being adopted to obtain cellulose products. For example, the Lyocell process utilizes the NMMO solvent to obtain regenerated cellulose fibers.<sup>9</sup> The Lyocell process is receiving considerable interest because of its environmentally friendly characteristics, simplicity, and the special properties of the resulting fibers. Compared to viscose fibers, the Lyocell fibers have higher tenacity, higher modulus, lower shrinkage in the dry state, and lower tenacity and modulus reduction in the wet state.<sup>10</sup>

While there has been considerable effort in obtaining fibers using cellulose solutions, reports describing the preparation of cellulose films are relatively scarce. Wu and Yuan<sup>6</sup> measured the gas permeability of dry as well as water-swollen cellulose films obtained by precipitating films of NMMO-cellulose solution in a water bath. The water-swollen films showed high  $\text{CO}_2/\text{N}_2$ ,  $\text{CO}_2/\text{CH}_4$ , and  $\text{CO}_2/\text{H}_2$  separation factors. Zhang and coworkers<sup>11</sup> measured the permeation of bovine serum albumin (BSA) through cellulose membranes prepared by coagulating films of NMMO-cellulose solution in aqueous NMMO-water baths. The scanning electron micrographs (SEMs) as well as pore size calculations indicate

either dense films or films possessing extremely small pores (pore size  $\sim$  15–40 nm). The researchers determined that BSA permeability decreased and BSA rejection increased with increasing solution cellulose concentration. Abe and Mochizuki<sup>12</sup> investigated the water permeation and sieving of dextran in flat hemodialysis membranes prepared from films of NMMO-cellulose solution coagulated in NMMO-water baths. While no morphological characteristics of the membranes were reported, our experience suggests that their casting protocols generated dense cellulose films. The authors indicate that water permeation increased with temperature and decreased with increasing cellulose concentration in the solution. In addition, they determined that the sieving coefficient (SC) for dextran (defined as the ratio of dextran concentration in the permeate to that in the feed solution) decreased with increasing temperature. However, the SC decrease was much less for smaller cellulose concentrations in the solution.

In contrast to the use of NMMO as a solvent, Zhou and coworkers<sup>13</sup> utilized an aqueous solution of urea and sodium hydroxide (NaOH) for dissolving regenerated cellulose. They prepared cellulose solutions by dissolving approximately 4.3 wt % cellulose polymer in a 6 wt % NaOH/4 wt % urea solution. Phase inversion was achieved by using aqueous  $\text{H}_2\text{SO}_4$  solutions of varying concentrations as the coagulation bath. SEM analysis indicated that the films had an isotropic structure with very small pores ( $<$  1  $\mu\text{m}$ ).

This literature review indicates that research has focused on dense films or films with very small pore sizes. Even for the dense films, the information available in the open literature is rather meager compared to that for cellulose derivatives such as CA. If native cellulose is to be treated as a more common

starting material for membrane formation, then protocols and methods to obtain porous cellulose films of specified pore size, porosity, and morphology need to be established. Clearly, the cellulose membrane morphologies reported to date do not seem suitable for NF, UF or MF separations.

In this work, we have focused our attention on fabrication of porous cellulose films with morphologies suitable for NF/UF applications. By a judicious selection of solvents, casting conditions, solution composition, and solvent exchange steps, we have successfully cast dense as well as skinned asymmetric porous cellulose films. In this paper, we present details of the casting process and the resulting film characteristics including mechanical properties,  $N_2$  permeability, and pore size/porosity.

## METHODS

### Materials and casting solution preparation

All membranes were prepared from a hardwood acetate grade dissolving cellulose supplied by Rayonier Performance Fibers, Inc in the form of flat sheets. After vacuum drying at 80°C, small pieces (~ 1 mm × 3 mm) cut from the sheets were used to prepare the cellulose solution. Solid NMMO (97%) obtained from Sigma-Aldrich was used as the starting material for preparation of the cellulose solvent. Since NMMO is hygroscopic and forms a stable complex with water, it was stored in a desiccator in a refrigerator. Whenever the NMMO bottle was opened, the space within the bottle was purged with dry  $N_2$  prior to closing. DMSO (analytical grade, Fisher) was the cosolvent, and was used as received; deionized (DI) water was used as a cosolvent for the NMMO. The polymer content ( $x$ ) was varied in the range 4–12 wt %, and the casting solution composition was  $x$  wt % cellulose, 45 wt % NMMO,  $(100 - x)$  wt % DMSO, and 5 wt % water. The water content of 5 wt % in the casting solution was chosen empirically, recognizing the fact that NMMO-water complexes (water : NMMO molecular ratio < 1) are direct solvents for cellulose.<sup>13</sup>

A clear homogeneous cellulose solution was obtained by adding the above components to a glass conical flask, and heating the flask in a silicone oil bath at 135°C under constant stirring for 20 min. At such a high temperature, degradation reactions occur that form several byproducts that, in turn, can provoke severe effects such as the degradation of cellulose, and accelerated decomposition of NMMO.<sup>14,15</sup> To prevent these side reactions and to stabilize the NMMO, a small quantity of propyl gallate (PG, Sigma-Aldrich, 97%, 0.005 g/g of cellulose) was added to the cellulose solution. Water evaporation from the casting solution during heating can change the composition of the casting solution and seemed

to adversely affect film morphology. Hence, evaporation of water was limited by piercing a Pasteur pipette through the septum that sealed the conical flask; the evaporated water condensed in the pipette and dripped back into the casting solution.

### Dense film casting

To obtain dense cellulose films, the cellulose solution was poured on a clean glass plate between 200- $\mu$ m steel shims, and a film was cast using a casting knife. The glass plate was then immersed in a DI water bath. Generally, the cellulose films peeled off the glass plate within 5 min of immersion. The films were washed by successively transferring them to two additional water baths for 30 min each, and finally stored in a third water bath overnight. The dense films so obtained were significantly swollen with water, and underwent significant shrinking and deformation upon drying. The dried films were extremely brittle, greatly distorted, and unsuitable for analytical testing. The shrinkage-induced deformation was prevented/minimized by using two different drying protocols:

1. After cutting off all the edges, the films were placed on glass plates and exposed to ambient conditions. Since the films adhered to glass strongly, they retained their flat shape even after the water had evaporated. When the corners started peeling, the glass plates were immersed in a water bath, and the films peeled off. These films were placed on paper towels, and after wiping off the excess water, kept in a vacuum oven at room temperature for 24 h. The residual stresses were relieved by placing the films in a vacuum oven at 110°C for 24 h. The dry film thickness was  $14 \pm 0.5 \mu\text{m}$ .
2. The films were transferred and stored in an isopropyl alcohol (IPA) bath for 24 h. Subsequently, slow drying was conducted by placing the films in a 1-mm gap between two glass plates and keeping them in a vacuum oven for 48 h at room temperature. Again the residual stresses were relieved by keeping the films in the vacuum oven at 110°C for 24 h. The dry film thickness was  $14 \pm 0.5 \mu\text{m}$ .

### Porous film casting

To obtain porous films, the glass plate was immersed in an acetone bath. Acetone is a nonsolvent for cellulose, and the ensuing mass transfer involving acetone, NMMO, DMSO, and water led to the formation of porous films. Due to the high surface energy of water, the pores invariably collapsed when the films were simply air-dried. To preserve the morphology, solvent exchange steps were incorporated into the protocol. After immersing the films

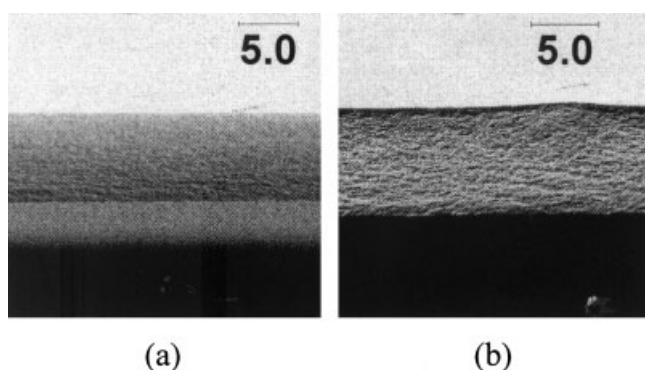


**Figure 2** SEM micrographs of the cross sections of two identical dense films obtained using a 4 wt % cellulose solution concentration and the following drying protocols: slow constrained air-drying (a) and IPA exchange followed by slow air-drying (b). Films of thickness  $14 \pm 0.3 \mu\text{m}$  could be reproducibly obtained, and no pores could be observed in the cross section within the resolution limit of the SEM ( $\sim 0.1 \mu\text{m}$ ). However, nitrogen permeation measurements suggested that the films might contain smaller pores, i.e., on the order of a few nanometers.

in acetone for 20 min, the films were placed in an isopropyl alcohol bath for 20 min. Subsequently, they were stored in a heptane bath for 24 h. The films were then dried by placing them on glass plates and exposing to dry ambient conditions. To ensure complete removal of residual solvent, the films were finally stored in a vacuum oven at  $80^\circ\text{C}$ .

### Cellulose film characterization

SEM analysis (Aspex Instruments, Tungsten filament with a 15 keV beam energy), tensile testing (Instron 8500 with a 5000 N load cell), and  $\text{N}_2$  permeability measurements were utilized to characterize the dense films. Cross sections of the dense films for SEM analysis were obtained by standard freeze-fracturing. For tensile testing, small strips ( $50 \text{ mm} \times 3 \text{ mm}$ ) of the dense films were attached to a specially designed fixture and extended under a constant rate of  $0.1 \text{ mm/s}$ . The force-elongation data were converted to corresponding engineering stress-strain values using the initial specimen dimensions, and the tensile modulus, failure stress, and failure strain were determined. The  $\text{N}_2$  permeability measurements were conducted using a custom permeation cell via the permeate pressure-rise technique. Details of the permeability apparatus and measurement technique are described in a previous paper.<sup>16</sup> Small circular samples (diameter: 25 mm) were placed in a permeation cell that was pressurized to 552 kPa (80 psi), and the rise in permeate pressure with time was recorded. The permeability of the films was then determined from these data.

The effect of the polymer concentration on the porous film morphology was studied by casting porous

films from 4, 7, and 11 wt % cellulose in the casting solution. The morphology was characterized in terms of the skin layer thickness, pore size distribution, and total porosity. Commercial image analysis software (Sigmascan) was used to obtain these three parameters from SEM micrographs of the film cross sections.

## RESULTS AND DISCUSSION

### Dense film studies

#### Microscopy

The dense films obtained by the aforementioned procedure were transparent and had a thickness of  $14 \pm 0.3 \mu\text{m}$ . Figure 2 shows SEM micrographs of typical dense film cross sections. The micrographs indicate the expected unremarkable film structure with no pores apparent within the resolution limit of the SEM ( $\sim 0.1 \mu\text{m}$ ). However, the films might still possess small pores of the order of a few nanometers. No evidence of significant differences in microstructure or thickness was obtained among the dense films obtained via the two drying protocols. We obtained good control over the final thickness of the films, which could be easily varied by using shims of different dimensions.

#### Mechanical property measurements

The tensile properties of the dense films were measured using a mechanical test system to ascertain the processability of the films in conventional fabrication equipment. For comparison, CA films fabricated in our laboratory via dry casting from a binary 15/85 wt % CA/Acetone solution were also tested. The measurements were conducted on 14 samples of cellulose films dried via Protocol 1, four samples of cellulose films dried via Protocol 2, and 10 CA film specimens. Table I summarizes the mechanical properties obtained including the tensile modulus ( $E$ ) and the stress ( $\sigma_f$ ) and strain ( $\epsilon_f$ ) at failure. The cellulose films dried via Protocol 2, i.e., initial immersion in an IPA bath followed by slow drying between two glass plates, evidenced higher ductility than those dried via Protocol 1. Since the films had been thoroughly dried to remove all of the volatile IPA, it is unlikely that residual solvent plasticized the films. We believe that the higher ductility of these films is caused by IPA conditioning. Since cellulose-water

**TABLE I**  
Mechanical Properties of Porous Cellulose and CA Films

Polymer	Tensile modulus (GPa)	Failure stress (MPa)	Failure strain (%)
Cellulose	$1.6 \pm 0.6$	$64.9 \pm 18.3$	$6.5 \pm 1.5$
CA	$2.0 \pm 0.6$	$60.1 \pm 11.6$	$13.1 \pm 8.0$



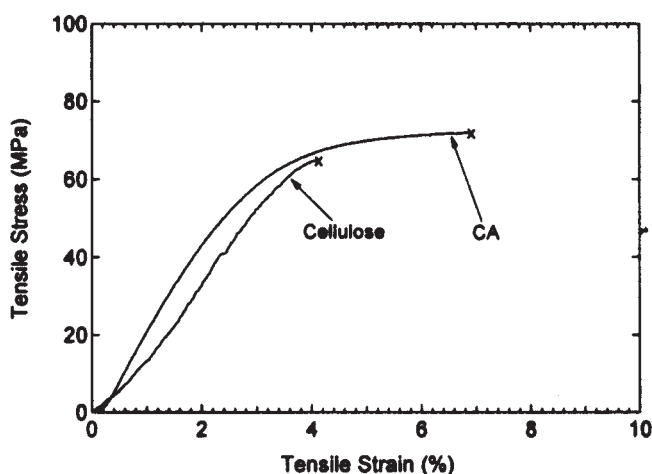


**Figure 3** Representative stress–strain responses of a cellulose and CA film: X indicates failure.

interactions are stronger than cellulose-IPA interactions (as reflected in the liquid retention values<sup>5</sup>), differences in the drying process likely produce differences in the inter- and intramolecular hydrogen bonding patterns for the cellulose hydroxyl group. A lower degree of intermolecular hydrogen bonding between the cellulose chains for the IPA-dried films could account for the higher ductility.

In general, the only significant difference in mechanical response of the specimens was the more brittle nature of cellulose as compared to the CA films (Fig. 3). This is expected, since cellulose films will have a significant degree of crystallinity, while CA has only limited crystallinity. The failure strain values in the range 5–10% agree with those reported in the literature for regenerated cellulose fibers.<sup>5</sup> The larger variability in the failure strain of the cellulose films appears to be caused by residual nonuniformity in the cellulose film samples. Despite the rigorous drying protocols employed, some of the films still contained small folds and creases. We observed that the more uniform cellulose samples evidenced somewhat greater failure stress and smaller failure strain values. Nonetheless, the mechanical property values obtained suggest that the dry cellulose films compare favorably to the CA films, and most likely possess sufficient mechanical integrity to enable processing on conventional fabrication equipment after casting and drying.

#### Gas permeability measurements

Prior to conducting nitrogen permeability measurements, the cellulose dense films were placed in the permeation cell and both sides of the films were exposed to nitrogen pressurized to 552 kPa (80 psi) for 12 h. Permeability testing was initiated after the films had been equilibrated with nitrogen in this fashion. Multiple permeability measurements were

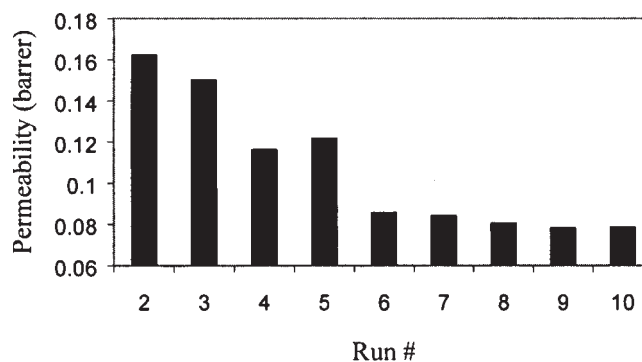


**Figure 4** Results of permeability measurements conducted on a single cellulose film sample. Successive measurements yielded progressively decreasing permeability values. However, film permeability attained a relative constant value after six successive runs. Consequently, 10 runs were conducted on each sample, and the mean of the final four runs was taken as the sample permeability.

performed on each cellulose film sample, since the film permeability was found to decrease with each progressive measurement. This suggests collapse of nanopores or the presence of residual solvent. Typical permeability values obtained on a single cellulose film are shown in Figure 4. Whereas the initial values were high, film permeability seemed to attain a constant value after six consecutive runs. Consequently, 10 successive measurements were conducted on each cellulose film sample. Figure 5 shows the consolidated nitrogen permeability data obtained from three films dried via Protocol 1 and Protocol 2, respectively, as well as three CA films. The data indicate that the film permeability depends upon the drying protocol. Films that were immersed in isopropyl alcohol prior to slow drying evidenced lower permeability values than did the films that were simply air-dried (Protocol 1). The relatively

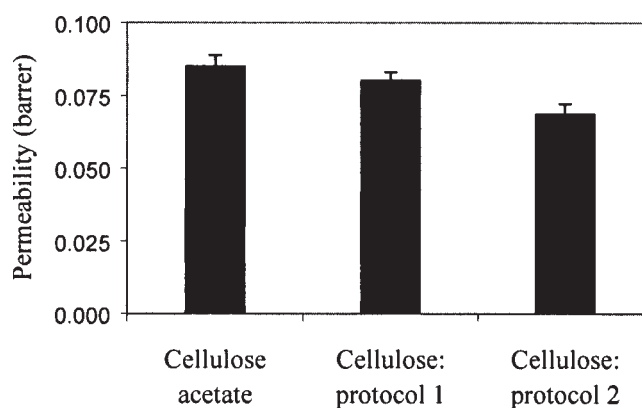


**Figure 5** Consolidated nitrogen permeability data obtained from three samples each of cellulose films dried via Protocols 1 and 2, as well as CA dense films. Cellulose films dried via Protocol 2 (isopropyl alcohol immersion prior to slow drying) evidence the lowest permeability values.

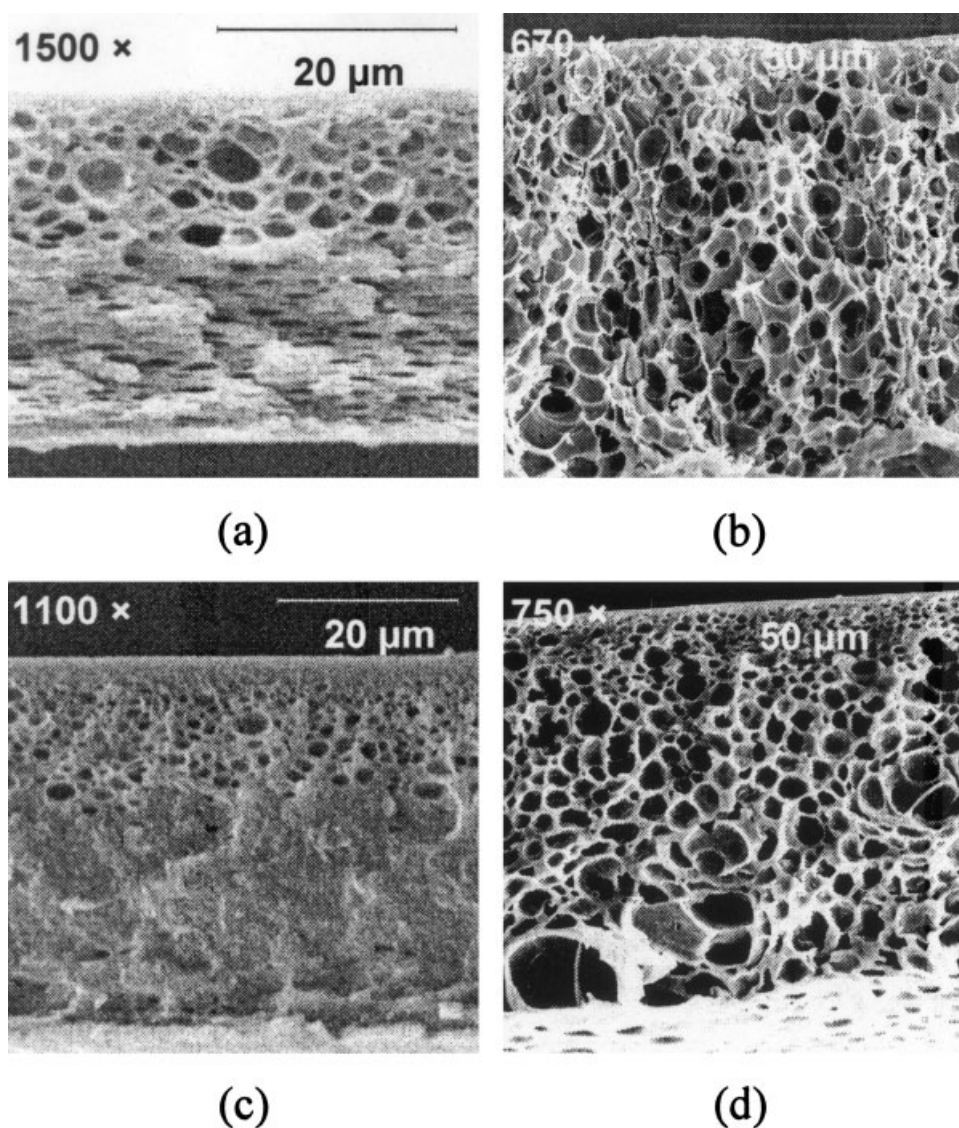


**Figure 6** SEM micrographs of porous film cross sections with (a and c) and without (b and d) water recycle during dissolution. For the films in (a) and (b), the solution contained 7 wt % cellulose, while for (c) and (d), the solution contained 10 wt % cellulose. The morphologies shown in (a) and (c) indicate that the loss of water via evaporation leads to pore collapse during drying.

modest difference may reflect small differences in the nanostructure or in the degree of crystallinity.

### Porous film studies

#### Effect of the presence of water on film morphology

Subtle variations in the composition of the ternary cellulose solvent system can have a significant effect on the morphology of the resulting cellulose films. Figure 6a shows the structure of a porous film that was cast from a cellulose solution in which the evaporated water was not recycled, i.e., returned to the solution. These films had a dense structure with small pores, in which the larger pores likely have collapsed. In contrast, when the evaporated water was returned to the casting solution, the films [Fig. 6(b)] had a well-defined

pore structure. While the exact mechanism for this behavior is unclear, we believe that the pore collapse is related to the kinetics of the phase inversion process. The solutions with slightly lower water content are in a “poorer” solvent for the cellulose polymer and thus precipitate more rapidly when immersed in the non-solvent bath. Pore collapse is generally associated with rapid phase inversion during the coagulation step,<sup>17–19</sup> whereas slow mass transfer in the solutions with high water content leads to the formation of a more spongy porous structure [Fig. 6(b)].

#### Effect of cellulose concentration on film morphology

Having established the importance of controlling the water concentration in the cellulose solvent system to

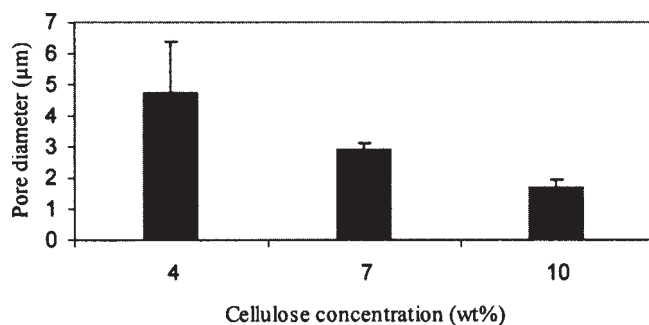


**Figure 7** Influence of the cellulose concentration in the solution on the mean pore diameter.

prevent pore collapse, we cast several porous films using water recycle during cellulose dissolution and studied the influence of cellulose solution concentration on the porous film morphology. As expected, the pore size as well as the porosity decreased with an increase in the casting solution cellulose concentration (Figs. 7 and 8). The lowest cellulose concentration of 4 wt % yielded films with large pores having a mean diameter of 4.8  $\mu\text{m}$ . The pore diameter monotonically decreased to 2.9  $\mu\text{m}$  and 1.8  $\mu\text{m}$  when the cellulose concentration was increased to 7 wt % and 10 wt %, respectively. Figure 9 shows the pore size distribution obtained from image analysis of multiple films at each cellulose concentration. The distribution was wide at a 4 wt % cellulose concentration due to the presence of large pores with diameters greater than 10  $\mu\text{m}$ . The distribution progressively became narrower with increasing cellulose concentration, indicating much smaller differences in the pore sizes. The similarity of the pore size distributions of multiple samples at the same solution cellulose concentration indicates the reproducibility of the porous film formation protocols. Thus, films with a mean pore diameter in the range 1.8–4.8  $\mu\text{m}$  can be produced by simply using a solution with the appropriate cellulose concentration.

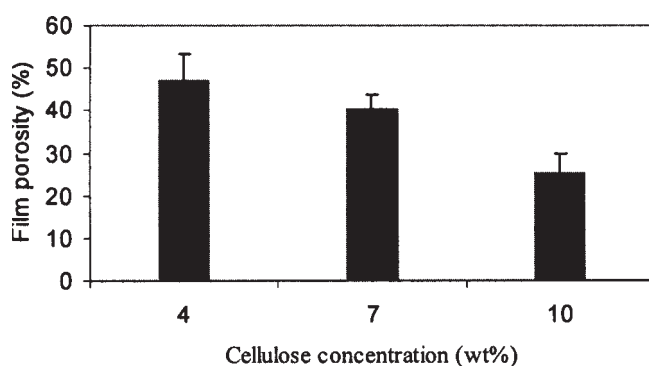
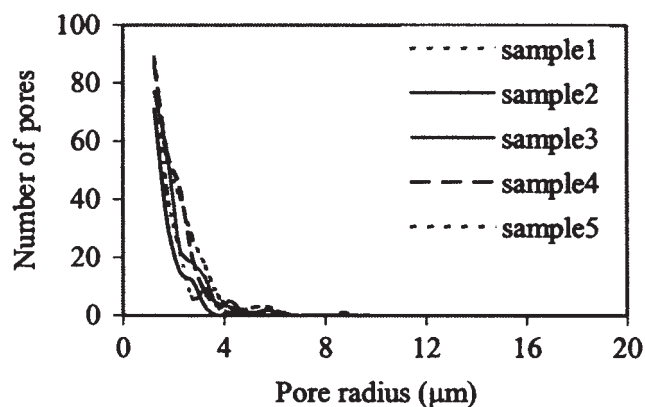
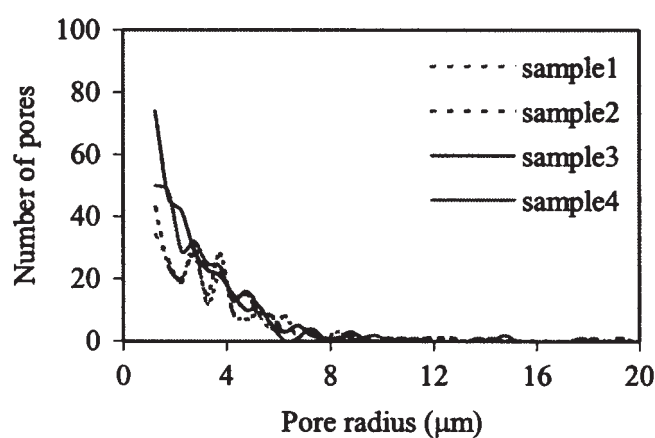


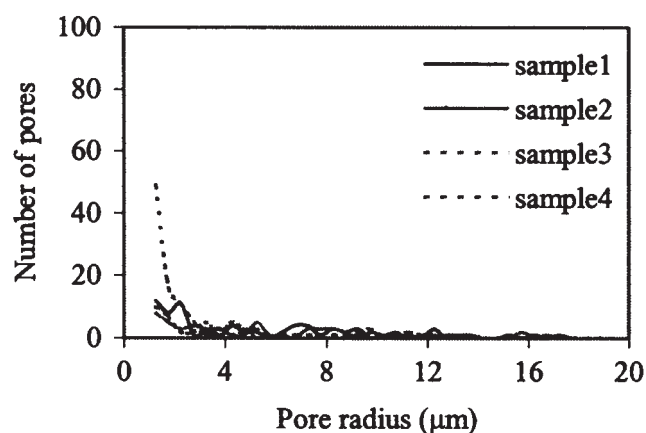
**Figure 8** Influence of the cellulose solution concentration on film porosity.



(a)



(b)



(c)

**Figure 9** Pore-size distribution graphs for porous films made from 4 wt % (a), 7 wt % (b), and 10 wt % (c) cellulose concentrations. The figures show a systematic decrease in the pore size with an increase in the cellulose concentration in the solution. At each concentration, tests were conducted on multiple films so that the reproducibility of the porous film formation protocol could be established.

Figure 10 shows the morphology of films made from the three cellulose solution concentrations. The cross section micrographs [Figs. 10(b,e,h)] reveal that



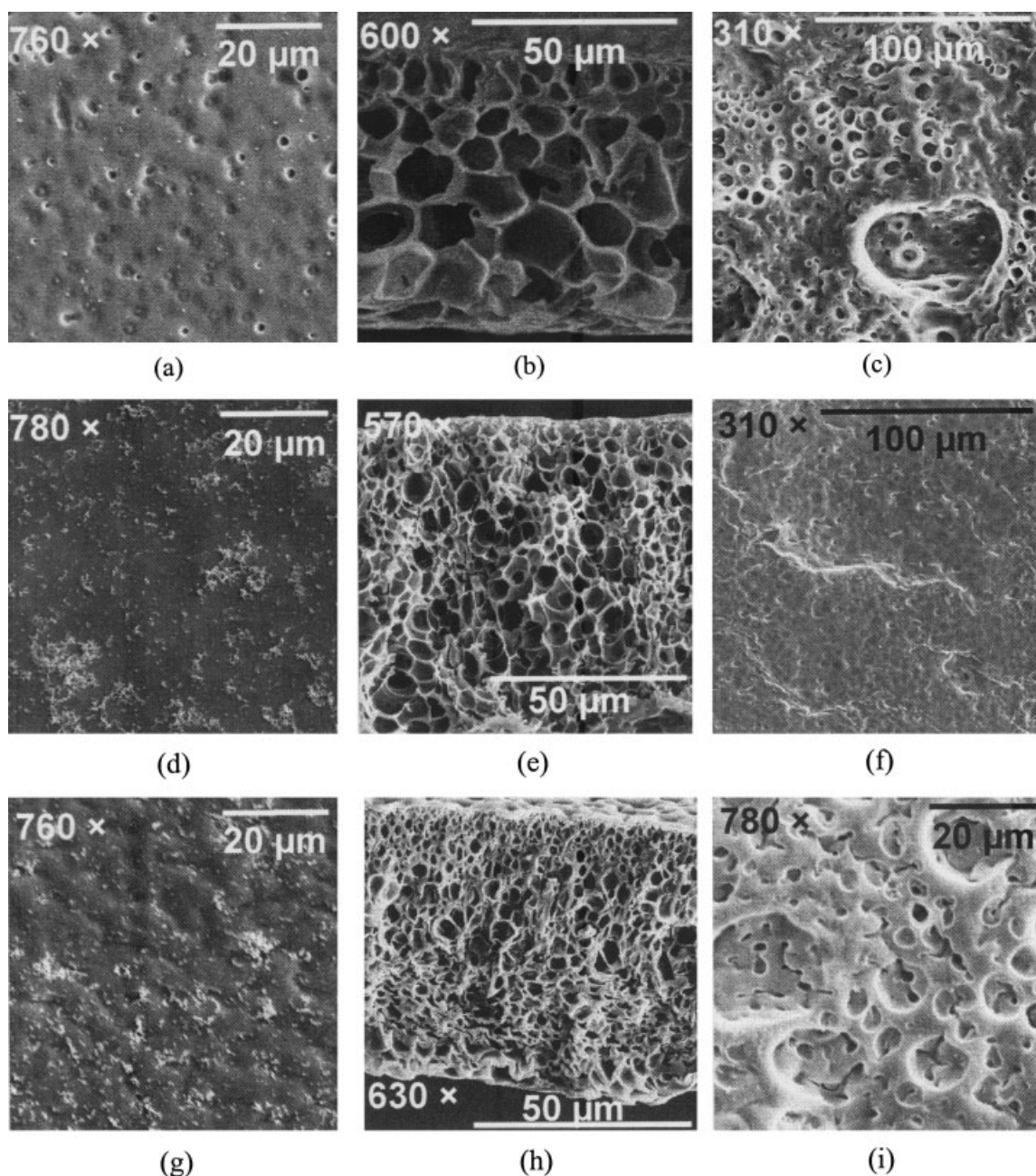


**Figure 10** SEM micrographs showing the morphology of cellulose films prepared from solutions with different cellulose concentrations. Figures (a), (d), and (g) correspond to the top surface of films cast using 4, 7, and 10 wt % cellulose in the solution, respectively. Likewise, Figures (b), (e), and (h) correspond to the cross section, and Figures (c), (f), and (i) correspond to the bottom surface at the three cellulose concentrations. The skin at the top surface is nonporous, and the micrographs indicate the precipitation of some polymer at the higher (7 and 10 wt %) cellulose concentration. The cross sections reveal a skinned asymmetric structure.

the porous films possess a skinned asymmetric structure, with small pores immediately beneath the skin, and pore size increasing away from the skin. Even though all of the films possessed a skin, the top surface of films made from 4 wt % cellulose concentration evidenced isolated small pores, probably formed because the thin skin layer is not strong enough to withstand the large interfacial stresses created during skin formation.

## CONCLUSIONS

The availability of new solvents such as NMMO, DMAc/LiCl, and 1-butyl-3-methylimidazolium chloride provides potential new routes for the synthesis of membranes directly from unmodified cellulose polymer. By using a judicious selection of solvents, cosolvents, nonsolvents and casting solution composition we were able to reproducibly cast dense films as well as porous cellulose films with mean pore



diameters in the range 1.8–4.8  $\mu\text{m}$ . Compared to dense CA films, the dense cellulose films were somewhat more brittle with similar  $\text{N}_2$  permeability values. Interestingly, the mechanical behavior depended upon the drying protocol employed, with films undergoing an IPA exchange step evidencing a slightly more ductile response. This dependence is most likely due to changes occurring in the hydrogen bonding at the intra- and intermolecular level during the drying process.

Subtle changes in the composition of the ternary cellulose solvent system significantly affected the porous structure. Porous films with a skinned asymmetric structure, and anisotropic porosity, i.e., small pores beneath the top skin and pore size increasing away from the skin, could easily be obtained. The mean pore size of these films can be altered by appropriate variation in the cellulose concentration of the casting solution.

Although the porous morphologies obtained would be suitable for ultrafiltration applications, some significant limitations for water-based uses exist since cellulose swells significantly in the presence of water and is especially susceptible to biological fouling. However, given the advantages of low cost and an environmentally friendly material, porous cellulose films might well find a niche in nonaqueous separation applications.

## References

1. Lloyd, D. R.; Meluch, T. B. In *Materials Science of Synthetic Membranes*; Lloyd, D. R., Ed.; ACS Symposium Series, 269, 1985.
2. Cardew, P. T.; Le, M. S. *Membrane Processes: A Technology Guide*; The Royal Society of Chemistry: Cambridge, 1998.
3. Koros, W. J.; Fleming, G. K. *J Membrane Sci* 1993, 83, 1.
4. Baker, R. W. *Membrane Technology and Applications*, 2nd ed.; John Wiley: West Sussex, UK, 2004.
5. Klemm, D.; Philipp, B.; T. Heinze, U.; Wagenknecht, W. *Comprehensive Cellulose Chemistry*, Vol. 1. Fundamentals and Analytical Methods, Wiley VCH: Germany, 1998.
6. Wu, J.; Yuan, Q. *J Membrane Sci* 2002, 204, 185.
7. Fink, H.-P.; Weigel, P.; Purz, H. P.; Ganster, J. *Prog Polym Sci* 2001, 26, 1473.
8. Swatloski, R. P.; Spear, S. K.; Holbrey, J. D.; Rogers, R. D. *JACS* 2002, 124, 4974.
9. Liu, R.; Shen, Y.; Shao, H.; Wu, C.; Hu, X. *Cellulose* 2001, 8, 13.
10. Peng, S.; Shao, H.; Hu, Z. *J Appl Polym Sci* 2003, 90, 1941.
11. Zhang, Y.; Shao, H.; Wu, C.; Hu, Z. *Macromol Biosci* 2001, 1, 141.
12. Abe, Y.; Mochizuki, A. *J Appl Polym Sci* 2002, 84, 2302.
13. Zhou, J.; Zhang, L.; Shu, H.; Chen, F. *J Macromol Sci Physics* 2002, B41, 1.
14. Biganska, O.; Navard, P. *Polymer* 2003, 44, 1035.
15. Rosenau, T.; Potthast, A.; Adorjan, I.; Hofinger, A.; Sixta, H.; Firgo, H.; Kosma, P. *Cellulose* 2002, 9, 283.
16. Reinsch, V. R.; Greenberg, A. R.; Kelley, S. S.; Peterson, R.; Bond, L. J. *J Membrane Sci* 2000, 171, 217.
17. Machado, P. S. T.; Habert, A. C.; Borges, C. P.; *J Membrane Sci* 1999, 155, 171.
18. Kang, Y. S.; Kim, H. J.; Kim, U. Y.; *J Membrane Sci* 1991, 60, 219.
19. Vandenburg, G. B.; Smolders, C. A. *J Membrane Sci* 1992, 73, 103.